Oil Shale, 2011, Vol. 28, No. 1S, pp. 169–180
doi: 10.3176/oil.2011.1S.09
ISSN 0208-189X

MATHEMATICAL MODEL OF TWO-PHASE FLOWS LOADED WITH LIGHT AND HEAVY PARTICLES TO ANALYZE CFB PROCESSES

A. KARTUSHINSKY[b]*, A. SIIRDE[a], Ü. RUDI[b], A. SHABLINSKY[a]

[a] Tallinn University of Technology
Faculty of Mechanical Engineering, Department of Thermal Engineering
Kopli 116, 11712 Tallinn, Estonia

[b] Tallinn University of Technology
Faculty of Science, Laboratory of Multiphase Media Physics
Akadeemia tee 15A, 12618 Tallinn, Estonia

Mathematical modeling of polydispersed (gas-solid particles) flow with light (ash) and heavy (corundum) particles is presented to analyze manifold process occurring in circulating fluidized beds (CFB). This study covers the process of turbulent mixing of particle and particle-particle collision, particle-surface collision and pertains the gravitation and viscous drag and lift forces. The 2D RANS (Reynolds Averaged Navier-Stokes) equations are used for numerical modeling of uprising polydispersed turbulent flow with implemented k-L_h model of closure. The flow domain is a round pipe with diameter of 30 mm and height of 100 calibers (pipe diameters). The flow (mean velocity up to 10 m/s) carries two fractions of ash particles (material density of 1020 kg/m^3 and sizes of 0.25 and 0.4 mm) and corundum particles (material density of 4000 kg/m^3 and size 0.4 mm). Two mass loadings – 5 and 10 kg/kg – were considered.

The results are presented in the form of distribution of axial and radial velocity components of gaseous and solid phases, particle mass concentration and kinetic turbulent energy along the flow height at steady-state flow cross-sections.

Introduction

This paper is a further development and analysis of the numerical modeling of the processes occurring in circulating fluidized beds (CFB). Within given numerical investigations we focus on the problem of turbulent motion of the particles along with particles' collision in the case of polydispersed solid

* Corresponding autor: e-mail *aleksander.kartusinski@ttu.ee*

admixture. The polydispersed admixture under study is a composition of light and heavy solid particles varying in size and rising up in the turbulent pipe flow. The first step is to evaluate the effect of variation in the particle material density on parameter distribution to develop further numerical modeling of such complicated flow in which heat conditions together with the real distribution of particle size and real composition of particle material occurring in real processes in CFB [1] will be included. The approach enables to optimize mass concentration of solid ash particles in fire gases. For the numerical simulation of the uprising gas-solid particle flow occurring in the vertical riser in the CFB conditions temperature, gas velocity, and particle concentration are followed. The particles of the Estonian oil shale ash are chosen.

The previous numerical simulations have been performed using the two-phase turbulent boundary layer (TBL) approach [2]. This approach implies that the diffusive source terms were retained only in one direction, namely in the transverse one, and magnitudes of the average transverse velocity components of the gaseous and dispersed phases were much less than those of the longitudinal components of the corresponding velocities of gaseous and dispersed phases. Such an approach is thoroughly valid and used in the case of pipe channel flows as well as in the case of turbulent round jets together with the flow past of the rigid shapes [3, 4].

In the present work we assess the mutual impact of two coexisting particle fractions, namely ash (light) and corundum (heavy) particles with variation in their particle sizes. The problem is solved by using the mathematical prediction (2D RANS) approach.

In comparison with our previous article, in calculations the following practical initial data [2] were used:

Table 1. **Initial data for calculations**

Parameter		Dimension	Minimal	Average	Maximal
Pipe data	Diameter	m	0.030	0.03	
	Height	m	3	3	
Ash concentration		kg/kg	5	10	0
Ash density		kg/m^3	1020	1020	0
Ash particle size		m	0.00025	0.0004	0.000
Corundum density		kg/m^3	4000	4000	0
Corundum particle size		m	0.00025	0.00025	0

The present research is a continuation of our previous numerical study of processes occurring in CFB using the two-fluid (Euler-Euler) approach describing the behavior of solid particles as a continuous co-existing solid phase. Along with this the 2D RANS modeling with the use of finite (control) volume method [5] is currently applied to avoid common assumptions of TBL approximation. We extended RANS modeling originally performed to model 2D the single-phase turbulent pipe flow for covering now a two-phase flow with an incorporated solid particle phase. The other popular approach now for modeling of the dispersed phase is the Lagrange particle tracking method. To use the Lagrange method, one can handle with huge number of tracking particles (up to several millions of particles depending on mass flow loading) to obtain solution convergence and to take into account particles' feedback into the primary (gas-phase) fluid, on the contrary to the Euler approach one can determine direct impact of particles on the fluid turbulent structure. The two-dimensional flow of gas-solid particles taking place in the CFB riser where the total volume concentration of solids is 3% was studied by the Lagrangian approach using the particles tracking method [6]. The Lagrangian approach of particle collisions was also used by Sommerfeld [7] who introduced a stochastic inter-particle model for the case when a fictitious particle and trace particles collide.

Theoretical terms of the model

As for multiphase flows, a lot of models were developed for particulate flows [8, 9]. The "two-fluid model" has been used at modeling dispersed two-phase systems, where the gas and the particles are considered to be two coexisting phases that reach the entire flow domain. To describe the flow of the particulate phase, one of the possibilities is using the Reynolds-Averaged Navier-Stokes (RANS) method. The general equations of this method were examined by plenty of experiments, which showed that using this method it is possible to discover, for example, boundary conditions, and it is quite easy to implement them numerically. In this work the RANS method is used for both coexisting phases, namely the gaseous and solid phases with closure equations. To close equations of both phases two approaches: a) Crowe model [9] to capture particle-turbulence interaction and b) Kartushinsky and Michaelides [10] particle collision model to assess inter-particle interaction were used to get needful data: axial and radial velocities, turbulent energy, mass concentration. The information on these parameters will surely be useful for particulate flow predictions.

Governing equations for the two dimensional RANS model

This model is based on the complete averaged Navier-Stokes equations applied for axi-symmetrical upward gas-solid particle turbulent pipe flow. The governing equations present the carrier fluid (gaseous phase) and solid (polydispersed) phase that are considered to be co-existing flow and consist of continuity equation for the gaseous phase and mass conservation equation for the dispersed phase together with momentum equations for both phases in streamwise and radial directions. In addition, the moment of momentum equation for the solid phase is included, because Magnus lift force and plausible particle rotation stem from the interaction with wall. The solid phase is considered to be a polydispersed phase with two particle fractions – light (ash) particles and heavy (corundum) particles. The system of governing equations is taken from the papers [11-13].

The system equations are presented in the tensor form with the following rule for indices variation: i = 1, 2; i = 1 = x; i = 2 = y; and i + 1 = 3 = x; summing over repeating indices.

Index "s" relates to the dispersed phase, and index "k" is number of particle fractions of the polydispersed phase, $1 \le k \le 2$.

1. Continuity for the gaseous phase:

$$\frac{\partial v_j}{\partial x_j} = 0$$

2. Momentum equation for the gaseous phase:

$$\frac{\partial}{\partial x_j}\left(v_i v_j + \overline{v_i' v_j'}\right) = -\frac{\partial p}{\rho \partial x_i} - \sum_{k=1,3} \alpha^k \left\{ \frac{v_{ri}^k}{\tau_k'} + (-1)^{i+1}\left[C_{Mi}^k \Omega^k + (i-1) F_s^k\right] v_{r(i+1)}^k \right\}$$

3. Closure equations for the gaseous phase (Boussinesq concept) and k-L Crowe model [10]:

$$\overline{v_i' v_j'} = -\nu_t \left(\frac{\partial v_i}{\partial x_j} + \frac{\partial v_j}{\partial x_i} \right) + \frac{2}{3} k \delta_{ij}$$

4. *Mass conservation equation of the dispersed phase:*

$$\frac{\partial \alpha^k v_{si}^k}{\partial x_i} = \frac{\partial}{\partial x_i}\left(D_t^k + D_s^k\right)\frac{\partial \alpha^k}{\partial x_i}$$

5. Momentum equation for the solid phase:

$$\frac{\partial}{\partial x_j} \alpha^k \left(v_{si}^k v_{sj}^k + \overline{v_{si}'^k v_{sj}'^k} \right)$$
$$= \alpha^k \left\{ \frac{v_{ri}^k}{\tau_k'} + (-1)^{i+1}\left[C_{Mi}^k \Omega^k + (i-1) F_s^k\right] v_{r(i+1)}^k - g\left(1 - \frac{\rho}{\rho_p}\right) \right\}$$

6. Linear momentum for the solid phase:

$$\frac{\partial}{\partial x_j} \alpha^k \left(\omega_{si}^k v_{sj}^k + \overline{\omega_{si}'^k v_{sj}'^k} \right) = \alpha^k C_\omega^k \frac{\Omega_i^k}{\tau'^k},$$

here p is pressure, v, v_s, and ω_s – linear and angular velocity components of gaseous and solid phases, respectively, and α – particle mass concentration. $v_{ri} = v_i - v_{si}$ is relative velocity of the dispersed phase, τ, τ' – particles' response time for Stokes and non-Stokes regimes, respectively. Coefficients C_{Mi} and F_{si} describe correction of the lift Magnus and Saffman forces, and $C_{\omega i}$ is rotation coefficient of particles taken from [14]. $\Omega = \text{rot}\vec{V} - \omega_s$ gives angular velocity slip of particles with average value, $\overline{v'^k_{si} v'^k_{sj}}$, and diffusion coefficients, D_t and D_s are the particles stress tensors. The average value represents the particle stress tensor components which are derived from inter-particle collisions. It describes diffusion of the particles from their collision. These solid phase parameters are calculated following the model of Kartushinsky and Michaelides [11]. For the calculation of the turbulent diffusion coefficient of particles the model Zaichik [15] is used.

Results and discussion

Numerical method. In the given RANS computations the *control volume* method was used. The governing equations (1–6) were solved using a strong implicit procedure with lower and upper matrix decomposition and with an up-wind scheme [5]. For the computations 280,000 uniformly distributed control volumes were run. Wall functions were incorporated at a dimensionless distance which has been taken as a half of the grid size from the wall.

All computations were extended from the pipe entrance to a distance up to *x/D* = 100. For the particulate phases in which the size of particles is often larger than the size of the viscous boundary sub-layer, the numerical method developed by Hussainov et al. was employed [3]. All results are presented in the dimensionless way: the velocities of both phases are related to gas-phase velocity at the flow center (*r* = 0), the turbulent energy – to square of gas-phase velocity at the flow center, the particle mass concentration – to its value at domain center of the flow (*r* = 0).

Numerical results. It is known that the increase in the particle mass concentration as well as the decrease in the particle size result in the decrease in the velocity slip between average velocities of gaseous and dispersed phases [3]. The effect of interparticle collisions is very important for the flows of particulates of the mass ratio larger than 1 (kg dust/kg air), when $\tau_c/\tau_p<1$, and the time of interparticle collision τ_c is less than the particle response time τ_p. We performed calculations taking into account the inter-particle collisions described by the analytically obtained stress tensor components $\overline{v'^k_{si} v'^k_{sj}}$ and calculation of diffusion coefficient D^k_s which is not empirical in equations (Eqs. (4–6)), they are obtained by analytical solution from an original model of closure given in [11].

The results of the simulation are shown in the following figures. In Fig. 1 there is axial velocity of carrier fluid (gaseous phase) and dispersed phase as a whole – average velocity of the mixture of ash and corundum solid particles is given as $\overline{u_s} = (\alpha_1 u_{s1} + \alpha_2 u_{s2})/(\alpha_1 + \alpha_2)$, where u_{s1} and α_1 are the axial linear velocity and particle mass concentration of the ash particle fraction, and u_{s2} and α_2 are the axial linear velocity and particle mass concentration of the particle fraction. The profile of axial velocity of the single phase is also shown in this figure. The two cases are examined, the flow with solid particles of ash of the same size, 250 microns, and with mass loading c=5 kg dust/kg air, and the mixture of larger ash particles, 400 microns and corundum particles 250 microns at higher mass loadings of c=10 kg/kg. The distribution of average velocity of the dispersed phase $\overline{u_s}$ is almost flat across the flow that differs from typical velocity profiles of the gaseous phase. The increase in mass loading and variation in particle size of solid admixture makes a small impact on the change of the shape of average velocity of the solid phase. The increased velocity close to the wall is due to higher rate of inter-particle collisions occurring in the solid mixture of ash and corundum particles of different particle sizes.

The axial velocity components of different solid particles are shown in Fig. 2. The particle velocity profiles are in consistence with their motion, so small and lighter ash particles move faster than corundum particles of the same mass of diameter 250 μ (see dashed bold and bold lines). This tendency is observed even for larger but lighter ash particles of 400 μ versus heavy smaller particles of 250 μ (see. dash-dotted and sold lines) at high mass loading of 10 kg/kg. However, we observe that in this case difference in velocity decreases.

Figure 3 shows distribution of radial velocity of gaseous and dispersed phases, namely profiles of ash and corundum particles plotted separately together with their average radial velocity which is calculated in the same manner as the previous axial velocity, $\overline{v_s}=(\alpha_1 v_{s1}+\alpha_2 v_{s2})/(\alpha_1+\alpha_2)$ for

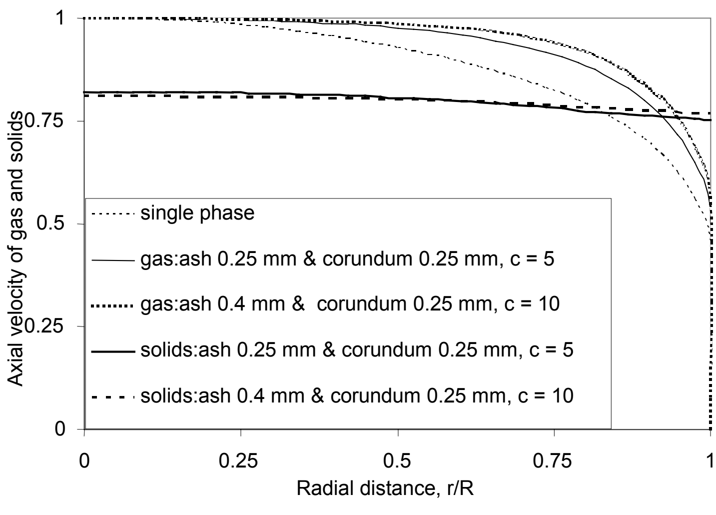

Fig. 1. Axial velocity distribution of gaseous and dispersed phases at different material densities and sizes: ash particles 0.25 mm and 0.4 mm, ρ_p = 1020 kg/m^3, corundum particles (0.25 mm and 0.4 mm, ρ_p = 4000 kg/m^3) and for two mass flow ratios: 5 and 10 kg/kg.

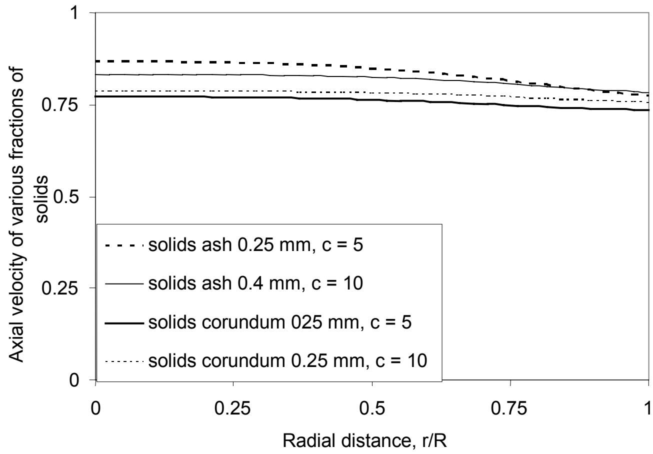

Fig. 2. Axial velocity profiles of ash and corundum particles at various particle size (0.25 and 0.4 mm) and mass loadings (c = 5 and 10 kg/kg).

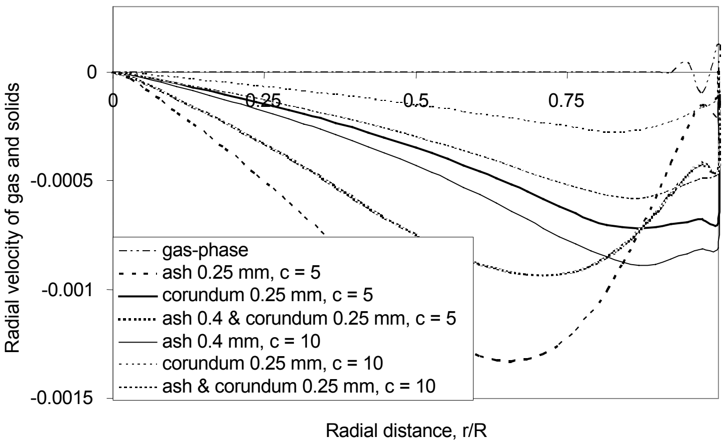

Fig. 3. Radial velocity profiles of gaseous and dispersed phases for ash and corundum particles of different sizes (0.25 and 0.4 mm) at various mass loadings (c = 5 and 10 kg/kg), and profiles of average radial of the mixture of solid components, $\overline{v_s}$ at various flow mass ratios (c = 5 and 10 kg/kg).

different mass loadings, c = 5 and 10 kg/kg, where v_{s1} is the radial linear velocity of the ash particle fraction and v_{s2} is the radial linear velocity of the corundum particle fraction. As one can see, magnitude of the radial velocity of the dispersed phase is larger than that of the gaseous phase. Besides, radial velocity of smaller and lighter ash particles is higher than that of heavy corundum particles (see bold dashed line and bold solid line). The increase in mass loading results in the decrease in radial velocity of the dispersed phase (see lines for average velocity $\overline{v_s}$ obtained for c = 5 and

10 kg/kg) which is associated with higher rate of turbulence attenuation observed for higher mass loading. The distribution of radial velocity of the dispersed phase is much more important because of its impact on the mixing process.

Figure 4 shows distribution of angular velocity of the dispersed phase for ash and corundum particles when the particles obtain rotation owing to their interaction with the pipe wall. As the figure shows, angular velocity gradually increases towards the wall, and rotation of light ash particles in the wall vicinity is higher than that of heavy corundum particles. Figure shows also average angular velocity calculated as previously for linear particle velocity components, $\overline{u_s}$ and $\overline{v_s}$, $\overline{\omega_s}=(\alpha_1\omega_{s1}+\alpha_2\omega_{s2})/(\alpha_1+\alpha_2)$, where ω_{s1} is the radial linear velocity of the ash particle fraction and ω_{s2} is the radial linear velocity of the corundum particle fraction. The rotation of the particles slows down due to inertia effect of corundum particles. The rotation of particles intensifies the process of mixing because of radial migration of particles across the flow.

Figure 5 shows distribution of turbulence energy in the single-phase pipe flow and in the gas-solid loaded pipe flows for different regimes: for the same particle size of ash and corundum of 250 μ at different mass loadings (c = 5 and 10 kg/kg) and for different particles sizes of ash of 400 μ and corundum of 250 μ at higher mass loading of 10 kg/kg. The whole trend shows that particles at all observed regimes attenuate turbulence almost along the entire cross-section, and they generate turbulence in the wall vicinity due to their small size and less inertia. According to Crowe criteria [10], the ratio of largest particle size (400 μ) to integral length scale is on the

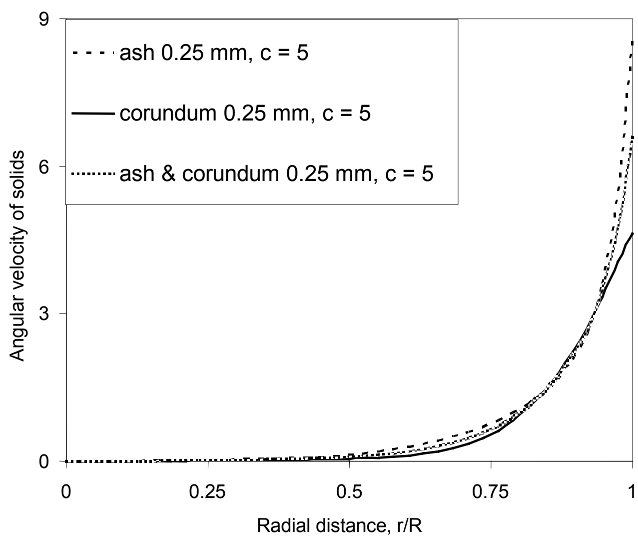

Fig. 4. Angular velocity profiles of ash and corundum particles (0.25 mm) and average profile of mixture of particles $\overline{\omega_s}$ at mass loading c = 5 kg/kg.

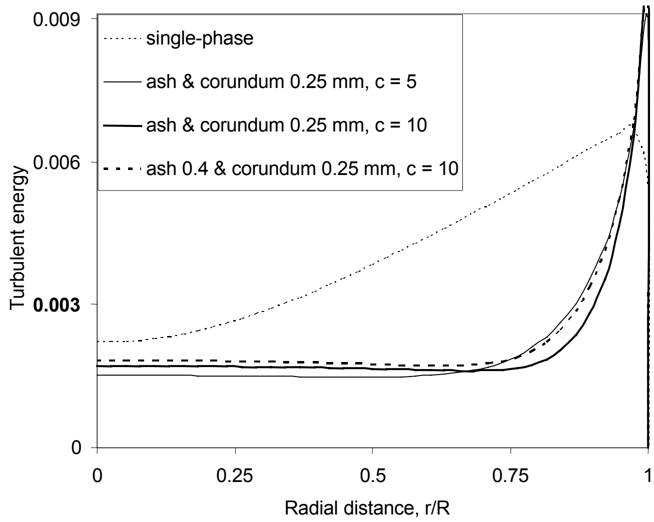

Fig. 5. Turbulent energy profiles of single and gaseous phases for the mixture of ash and corundum particles of the same size of 0.25 mm. Flow mass ratios c = 5 and 10 kg/kg, mixture of ash and corundum with different particle size: ash 0.4 mm and corundum 0.25 mm for mass flow ratio c = 10 kg/kg.

domain where particles should damp turbulence, or it lays close to the edge of turbulence attenuation/generation effect by the presence of particles. The increase in polydispersity (variation of particle size 400 μ of ash and 250 μ of corundum together with variation of particle material density) raises the level of turbulence in the two-phase flow (see dashed bold line and solid bold line). Such a tendency is observed for the increase in the mass flow ratio (see solid line and bold solid line in Fig. 5). To enhance turbulence, it would be better to use larger particles such as at least double their size which probably occurs in a real process, for example in CFB (circulating fluidized bed). Higher turbulence level leads to better mixing and thus to higher efficiency of the combustion process in CFB.

Finally, Fig. 6 shows distribution of particle mass concentration across the flow in the tested flow regimes. All cases show a general tendency of the decrease in mass concentration towards the wall because of higher gravitation and less axial velocity component of the dispersed phase near the wall. Mass concentration of light ash particles of average concentration $\overline{\alpha}=\alpha_1+\alpha_2$ and corundum particles of 250 μ near the wall is less than that of particles of high polydispersity of different particle size (400 μ for ash and 250 μ for corundum). The increase in flow mass ratio is less pronounced than variation in particle size. Particle size distribution is also a very important factor in determining CFB efficiency. The gradient profiles of mass concentration may show obstacles in the combustion process, therefore one has to know corundum mass fraction distribution to improve combustion cycles.

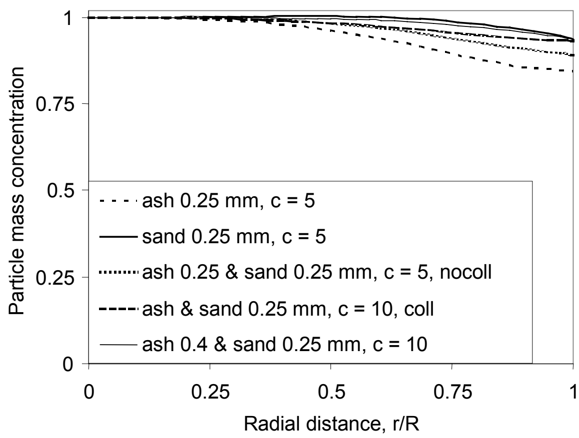

Fig. 6. Distribution of particle mass concentration for mixture components: ash and corundum particles of 0.25 mm at mass ratios c = 5 and 10 kg/kg, average mass concentration $\overline{\alpha}$ for the same (ash and corundum 0.25 mm) and different particle sizes (ash 0.25 and corundum 0.4 mm) at mass ratio c = 5 kg/kg (without collision of particles) and c = 10 kg/kg (with collision of particles).

Comparison of the results

Comparing the results with those of our previous work "Numerical simulation of uprising gas-solid particle flow in circulating fluidized bed", in which theoretical initial data was used, the following remarkable facts can be marked:

– the presence of the other fraction – heavier particles of corundum – and the numerical results obtained are compared with our previous results. Calculations considering two particle fractions in the flow reflect more truly the actual process occurring in CFB.
– the results describe more qualitatively the processes analogous to the actual processes in real objects in terms of geometry of CFB units showing that involvement of the other particle fraction may noticeably modify the whole process in CFB.

Conclusions

The numerical simulation of the two-phase fluid dynamics performed by Euler/Euler (2D RANS) approach showed the importance of involvement of a second solid fraction (ash and corundum particles) in formation of the whole process occurring in CFB. The main contributors to the formation of the flow are interparticle collisions and modulation of the four-way coupling turbulence due to the presence of solids. The other forces affecting the motion of solids are gravitation, viscous drag and lift forces. On the basis of the performed calculations we can conclude that the presence of the other fraction results in:

a) decrease in elevation rate of motion of the polydispersed phase along with the velocity of carrier fluid;
b) variation in particle size in the polydispersed admixture that decreases its radial velocity and increases turbulence level due to inter-particle collisions;
c) variation in particle size in the polydispersed admixture that results in aligning the profiles of mass concentration in flow cross-sections because of high dispersion rate.

The obtained results can be used for real-scaled CFB risers with solid ash particles of Estonian shale if the size of two main particle fractions will be increased.

REFERENCES

1. *Ots, A*. Oil Shale Fuel Combustion. – Tallinn, 2006. 833 pages.
2. *Kartushinsky, A., Martins, A., Rudi, Ü., Shcheglov, I., Tisler, S., Krupenski, I., Siirde, A*. Numerical simulation of uprising gas-solid particle flow in circulating fluidized bed // Oil Shale. 2009. Vol. 26, No. 2. P. 125–138.
3. *Hussainov, M., Kartushinsky, A., Mulgi, A., Rudi, Ü*. Gas-solid flow with the slip velocity of particles in a horizontal channel // J. Aerosol. Sci. 1996. Vol. 27, No. 1, P. 41–59.
4. *Frishman, F., Hussainov, M., Kartushinsky, A., Mulgi, A*. Numerical simulation of a two-phase turbulent pipe-jet flow loaded with polydispersed solid admixture // Int. J. Multiphas. Flow. 1997. Vol. 23, No. 4. P. 765–796.
5. *Ferziger, J. H., Perić, M*. Computational Methods for Fluid Dynamics. – New York: Springer-Verlag, 1995. 356 p.
6. *Helland, E., Occelli, R., Tadrist, L*. Numerical study of cluster formation in a gas-particle circulating fluidized bed // Powder Technol. 2000. Vol. 110, No. 3. P. 210–221.
7. *Sommerfeld, M*. Validation of a stochastic Lagrangian modelling approach for inter-particle collisions in homogeneous isotropic turbulence // Int. J. Multiphas. Flow. 2001. Vol. 27, No. 10. P. 1829–1858.
8. *Pfeffer, R., Rosetti, S. Licklein, S*. Analysis and correlation of heat transfer coefficient and friction factor data for dilute gas–solid suspensions. – NASA rep. TND-3603, 1966.
9. *Michaelides, E. E*. A model for the flow of solid particles in gases // Int. J. Multiphas. Flow, 1983, Vol. 10, No. 1. P. 61–77.
10. *Crowe, C. T*. On models for turbulence modulation in fluid-particle flows // Int. J. Multiphas. Flow. 2000. Vol. 26, No. 5. P. 719–727.
11. *Kartushinsky, A., Michaelides, E. E*. An analytical approach for the closure equations of gas-solid flows with inter-particle collisions // Int. J. Multiphas. Flow. 2004. Vol. 30, No. 2. P. 159–180.
12. *Kartushinsky, A., Michaelides, E. E*. Particle-laden gas flow in horizontal channels with collision effects // Powder Technol. 2006. Vol. 168, No. 2. P. 89–103.

13. *Kartushinsky, A., Michaelides, E. E., Hussainov, M. T., Rudi, Y.* Effects of the variation of mass loading and particle density in gas-solid particle flow in pipes // Powder Technol. 2009. Vol. 193, No. 2. P. 176–181.
14. *Michaelides, E. E.* Particles, Bubbles & Drops: Their Motion, Heat and Mass Transfer. – World Scientific Publishers, New Jersey, 2006.
15. *Zaichik, L. I., Alipchenkov, V. M.* Statistical models for predicting particle dispersion and preferential concentration in turbulent flows // Int. J. Heat Fluid Flow. 2005. Vol. 26, No. 3. P. 416–430.

Received December 2, 2010